

Recommended vapor pressure and thermophysical data for ferrocene

Michal Fulem^{a,b,}, Květoslav Růžička^a, Ctirad Červinka^a, Marisa A.A. Rocha^c, Luís M. N.*

B. F. Santos^c, Robert F. Berg^d

^a Department of Physical Chemistry, Institute of Chemical Technology, Prague, Technická 5,
CZ-166 28 Prague 6, Czech Republic

^b Department of Semiconductors, Institute of Physics, Academy of Sciences of the Czech
Republic, v. v. i., Cukrovarnická 10, CZ-162 00 Prague 6, Czech Republic

^c Centro de Investigação em Química, Departamento de Química e Bioquímica, Faculdade de
Ciências da Universidade do Porto, Rua do Campo Alegre, 687, P-4169-007 Porto, Portugal

^d Sensor Science Division, National Institute of Standards and Technology, Gaithersburg,
Maryland 20899, U.S.A.

*Corresponding author: fulemm@vscht.cz

Abstract

Recommended vapor pressure data for ferrocene (CAS Registry Number: 102-54-5) in the temperature range from 242 to 447 K were developed by the simultaneous correlation of critically assessed vapor pressures, heat capacities of the crystalline phase and the ideal gas, and calorimetrically determined enthalpies of sublimation. All of the properties needed for the correlation were newly determined in this work. The value for the enthalpy of sublimation, $\Delta_{\text{cr}}^{\text{g}}H_{\text{m}}$ (298.15 K) = (74.38 \pm 0.38) kJ·mol⁻¹, is recommended. Comparisons with literature values are shown for all measured and derived properties.

Keywords: ferrocene; vapor pressure; heat capacity; ideal gas thermodynamic properties; sublimation enthalpy; recommended vapor pressure equation

1. Introduction

Ferrocene is a good candidate for calibrating vapor pressure experimental apparatus [1], and ICTAC recommends it as a primary standard for sublimation enthalpy [2]. However, the ICTAC recommendation was based mainly on Clausius-Clapeyron calculations from vapor pressure data with empirical corrections [3]. The scatter of the resulting values span a range of approximately 5 kJ·mol⁻¹, which is much greater than the experimental uncertainty.

This work presents a joint effort of three laboratories (ICT Prague, University of Porto, and NIST) to develop improved thermophysical property data for ferrocene. Calculated ideal gas heat capacities and critically assessed experimental data for vapor pressure, crystalline heat capacity, and enthalpy of sublimation were treated simultaneously to obtain a consistent thermodynamic description. All of the thermophysical properties needed as input for the simultaneous correlation were newly determined in this work. The measurements were performed with the same sample of ferrocene, which was purified by vacuum sublimation and

then distributed among the three laboratories. Vapor pressures were measured using the static method with two apparatuses over the temperature range from 288 to 452 K. Heat capacities of the crystalline phase were determined by Calvet and drop calorimetry. The direct measurements of enthalpies of sublimation were carried out by using a Calvet microcalorimeter. The thermodynamic properties of the ideal gas state were calculated by combining statistical thermodynamics, density functional theory (DFT) calculations, and the only experimental value [4] for the barrier to internal rotation of cyclopentadienyl rings.

2. Simultaneous treatment of vapor pressures and related thermal data (SimCor method)

The vapor pressure p , the sublimation enthalpy $\Delta_{\text{cr}}^{\text{g}}H_{\text{m}}$, and the difference $\Delta_{\text{cr}}^{\text{g}}C_{p,\text{m}} = C_{p,\text{m}}^{\text{g}} - C_{p,\text{m}}^{\text{cr}}$ between the heat capacities of the saturated gas $C_{p,\text{m}}^{\text{g}}$ and the crystalline solid $C_{p,\text{m}}^{\text{cr}}$ are linked by the exact thermodynamic relationships:

$$\Delta H' \equiv \Delta_{\text{cr}}^{\text{g}}H_{\text{m}} / \Delta_{\text{cr}}^{\text{g}}z = RT^2(d \ln p / dT)_{\text{sat}} \quad (1)$$

and

$$\begin{aligned} \Delta C' \equiv (d\Delta H' / dT)_{\text{sat}} &= R \left\{ d \left[T^2 (d \ln p / dT) \right] / dT \right\}_{\text{sat}} = \\ &= \left[\Delta_{\text{cr}}^{\text{g}}C_{p,\text{m}} - 2\Delta H' \left(\partial \Delta_{\text{cr}}^{\text{g}}z / \partial T \right)_p - \frac{P}{RT} \Delta H'^2 \left(\partial \Delta_{\text{cr}}^{\text{g}}z / \partial p \right)_T \right] / \Delta_{\text{cr}}^{\text{g}}z \end{aligned} \quad (2)$$

Here, the subscript 'sat' denotes a derivative along the saturation line, R is the molar gas constant, T is the temperature, and $\Delta_{\text{cr}}^{\text{g}}z$ is the difference between the compressibility factors of the coexisting phases. The auxiliary quantities $\Delta H'$ and $\Delta C'$ can be calculated using equations (1) and (2), either from the vapor pressure correlating equation $p(T)$ (by substituting the derivative $d \ln p / dT$), or from experimental values of sublimation enthalpy $\Delta_{\text{cr}}^{\text{g}}H_{\text{m}}$ and $\Delta_{\text{cr}}^{\text{g}}C_{p,\text{m}}$ calculated from experimental data by combining calculated values of ideal gas heat capacities $C_{p,\text{m}}^{\text{g}0}$, calorimetric values of $C_{p,\text{m}}^{\text{cr}}$, and pVT data for the saturated gas whose

importance, however, decreases rapidly as the temperature (pressure) is reduced (for more details, see [5, 6]). This means that, after selecting a suitable description of $p(T)$, it is possible to correlate simultaneously experimental values of p , $\Delta_{\text{cr}}^{\text{g}}H_{\text{m}}$ and $\Delta_{\text{cr}}^{\text{g}}C_{p,\text{m}}$ as a function of temperature.

The Cox equation is among the best correlating equations for describing simultaneously vapor pressure and related thermal data as a function of temperature down to the triple point [7]. It has the form [8]

$$\ln \frac{p}{p^0} = \left(1 - \frac{T^0 / \text{K}}{T / \text{K}}\right) \exp\left(\sum_{i=0}^n A_i (T / \text{K})^i\right), \quad (3)$$

where T^0 and p^0 are the temperature and pressure of an arbitrarily chosen reference point and the A_i are correlation parameters. $n = 2$ is usually adequate; fewer parameters can be used when the temperature range is narrow, and more can be used when the temperature range is wide or when the temperature dependence of $\Delta_{\text{cr}}^{\text{g}}C_{p,\text{m}}$ is complex.

The SimCor method used here has been thoroughly tested [7], and it has been used previously to obtain recommended vapor pressure for several crystalline and liquid compounds [9-16].

3. Experimental Section

3.1. Materials. The sample description is given in table 1. After the purification by vacuum sublimation the sample was distributed among the three laboratories, and two independent purity analyses were performed.

3.2. Vapor pressure measurements.

3.2.1. ICT Prague

The apparatus described in [17] was used to thoroughly degas the sample by direct pumping with a turbomolecular vacuum pump for two weeks at approximately 298 K. The vapor pressure measurements at ICT were performed using the static method with the previously described STAT6 apparatus [18], and thus only a short description is needed here. The apparatus was constructed of electrochemically polished stainless steel tubing, metal-gasketed connections (ConFlat DN 16 CF and VCR [19]), and all-metal, pneumatically operated, angle valves designed for ultra-high vacuum (series 57, VAT Vacuumvalves AG, Switzerland).

The pressure was measured simultaneously by two absolute capacitance diaphragm gauges (CDGs) that were kept at 318 K by an internal temperature controller (Baratron 690A01TRA (133 Pa), Baratron 690A11TRA (1333 Pa), MKS Instruments, USA). The manufacturer calibrated the CDGs at 318 K over their full ranges at 11 equally spaced pressures with a maximum relative deviation of 0.03 %; those calibrations were traceable to NIST. The Czech Metrology Institute performed additional calibrations at $p_{\text{CDG}} < 10$ Pa with a standard uncertainty of $u(p_{\text{CDG}}) = 0.0005p_{\text{CDG}}$. The additional calibrations agreed with the manufacturer's calibration, and they extended the useful ranges to pressures below the manufacturer's calibration. The sample temperature was measured by a four-wire platinum resistance thermometer that had been calibrated by the manufacturer at the ice point and/or by comparison to a standard platinum resistance thermometer whose calibration was traceable to NIST. The resulting standard uncertainty of the sample temperature was $u(T) = 0.02$ K, which is insignificant in the pressure range investigated in this work. All temperatures reported here are based on the international temperature scale ITS-90.

The performance of the apparatus was checked by measurements of naphthalene, which is recommended for calibrating vapor pressure apparatus [15]. The agreement with the recommended data [15] was within the standard uncertainty of the STAT6 apparatus, which is adequately described by $u(p) = 0.005p + 0.05$ Pa.

The vapor pressure measurements of ferrocene were performed in the temperature interval from 288 K to 311 K by varying the temperature at random to detect systematic errors caused by insufficient degassing of the sample. The experiments were carried out repeatedly at selected temperatures. When the pressure change was negligible with the number of measuring cycles, the sample was considered completely degassed, and the final set of data was recorded. At least two experimental points were obtained for each temperature.

3.2.2. NIST

The vapor pressure measurements at NIST also used the static method, but they differed from those made at ICT in three ways.

1. The temperature range extended up to the triple point at 447 K.
2. The temperature of the pressure gauges was allowed to vary. Keeping them 1 K warmer than the sample prevented condensation in the gauges.
3. The sample was degassed after it was put into the vapor pressure apparatus.

This section describes briefly the construction and operation of the NIST apparatus; a longer description is in preparation [20].

The apparatus had a “hot” gas manifold contained in a convection oven and a “cold” manifold at room temperature. The hot manifold comprised the sample tube, two CDGs, and a cold trap that were connected by pneumatic valves and metal gasket fittings (1/4 inch VCR [19]). The sample tube was constructed by welding an end cap and a VCR fitting onto a thin-walled, stainless steel tube. The CDGs (MKS model 616) were differential pressure gauges with ranges of 1.3 kPa and 130 kPa, and the pneumatic valves (Fujikin FWB(R)-71-6.35-2) were all-metal diaphragm valves. Both were designed to operate at temperatures as high as 573 K. The cold trap was a U-shaped length of stainless steel bellows. The volume of the hot manifold was 29 cm³.

The sample tube was surrounded by an aluminum block fitted with a thermistor, a platinum resistance thermometer (PRT), and two thermoelectric elements. The thermoelectric block kept the temperature of the sample tube 1 K colder than that of the oven. As described in [21] this device can operate at temperatures as high as 473 K while controlling the sample with a precision of 0.02 K; below 383 K the precision is 2 mK. The uncertainty of the sample temperature, which was dominated by that of the PRT, was less than 0.012 K.

The cold manifold comprised a quartz flexure pressure gauge, a turbo-drag vacuum pump, a zeolite-filled trap, connections for air and nitrogen gas, and a burner tube for decomposing vapors released from the trap. The pressure gauge had a full scale of 310 kPa, a resolution of 1 Pa, and a long-term stability of 31 Pa. It was calibrated against a vacuum-referenced piston gauge over the range from 2 kPa to 208 kPa. We extrapolated the calibration to pressures below 2 kPa by assuming that the gauge's reading was a linear function of pressure. This assumption was verified by plotting the CDG reading as a function of the quartz gauge reading; the deviations from a linear fit were smaller than 1 mPa.

Before loading the sample, the apparatus was baked and pumped for two weeks at 523 K. Due to the release of hydrogen from the stainless steel, this baking was much longer and hotter than needed to remove water and hydrocarbons. Hydrogen outgassing is not a concern for measuring vapor pressures above 1 Pa when the temperature is below 373 K. However, at 473 K the hydrogen outgassing could increase the pressure in the empty manifold as fast as 0.5 Pa min⁻¹; the baking reduced that rate by a factor of 100.

The performance of the apparatus was checked by measurements of the vapor pressure of naphthalene, for which there are reliable literature [15].

Approximately 1 g of the purified sample was sealed into the sample tube, which was then attached to the manifold in the oven. The initial degassing procedure used intermittent pumping, in which the sample tube was cyclically opened to the hot manifold and the rate of pressure increase dp/dt was measured for 1-2 hr, after which the sample tube was closed and

the manifold was evacuated. After approximately 100 such cycles at either 352 K or 382 K, the sample was degassed further by subliming it from the sample tube at 382 K to the trap at 273 K while pumping through the trap. Calculations based on Raoult's law and a rough estimate of the diffusivity of nitrogen suggested that these procedures should have reduced the outgassing of air to a negligible level. Instead, dp/dt was reduced to a level that was nonzero but sufficiently small for measuring the vapor pressure.

The temperature was cycled five times in a series of steps; each cycle included most or all of the range from 302 K to 452 K. At each temperature, the valves were cycled from 3 to 30 times to (1) measure the CDG voltage $V_{\text{CDG}}(p)$, (2) evacuate the hot manifold, and (3) measure the voltage at zero pressure $V_{\text{CDG}}(0)$. Usually, the value of $V_{\text{CDG}}(p)$ slowly increased after the sample tube was opened, and this was attributed to the diffusion of a volatile impurity out of the sample. Therefore, only the value measured immediately after opening the sample tube was used. The vapor pressure $p(T)$ was determined by multiplying the voltage difference by a calibration factor:

$$p = [V_{\text{CDG}}(p) - V_{\text{CDG}}(0)] \times (\text{CDG calibration factor}). \quad (4)$$

The CDGs were calibrated by comparing them to the quartz flexure pressure gauge; this was done each time after the hot manifold was baked. The calibration procedure included setting the oven at a series of temperatures $293 \text{ K} < T < 473 \text{ K}$ and using nitrogen to vary the pressure from zero to full scale at each temperature. (Thermal transpiration caused negligible error because the lowest calibration pressure was 200 Pa.) The resulting difference between the calibration pressure p and the nominal CDG reading p_{nom} was expressed as a cubic polynomial of p_{nom} with coefficients $k_i(T)$ that were quadratic polynomials of T .

$$p - p_{\text{nom}} = k_0(T) + k_1(T)p_{\text{nom}} + k_2(T)p_{\text{nom}}^2 + k_3(T)p_{\text{nom}}^3 \quad (5)$$

The temperature cycles during the measurements of vapor pressure caused small but significant changes of the CDG zero k_0 and the CDG linear coefficient k_1 . The value of k_0 was obtained at each temperature step from the multiple measurements $V_{\text{CDG}}(0)$. The value of k_1

was measured at the end of each temperature step by closing the sample tube and running an incomplete calibration with nitrogen that spanned less than 30 % of the CDG's full scale pressure.

3.3. Heat capacity measurements.

3.3.1. ICT Prague

The heat capacity was measured at ICT with a Calvet calorimeter (Setaram μ DSC IIIa, France) in the range from 273 to 355 K and used the incremental temperature mode (step method) [22]. Each 5 K step included a heating rate of 0.5 K min^{-1} followed by an isothermal delay of 3600 s. The mass of the sample, as determined by an analytical balance with a readability of 0.01 mg, was 720.49 mg. The combined expanded uncertainty of the ICT heat capacity measurements is estimated to be $U_c(C_{p,m}) = 0.01 C_{p,m}$. A detailed description of the calorimeter and its calibration can be found in a paper by Straka et al. [23]; the measuring procedure was described in detail in [24].

3.3.2. University of Porto

The heat capacity of the crystalline phase was also measured at $T = 298.15 \text{ K}$ using a non-commercial high-precision drop calorimeter (University of Porto) and the drop method, which is described in detail in [25-27]. The apparatus comprises two main parts: a furnace for temperature equilibration of the sample ampoule and calorimetric receiving block based on a twin heat conduction type. The calorimeter was calibrated with water and sapphire ($\alpha\text{-Al}_2\text{O}_3$ pellets, NIST SRM 720) based on a $\Delta T = 10 \text{ K}$ drop procedure, using the respective standard molar heat capacities at 298.15 K reported in the literature, $C_{p,m}(\alpha\text{-Al}_2\text{O}_3) = (79.03 \pm 0.08) \text{ J}\cdot\text{K}^{-1}\cdot\text{mol}^{-1}$ and $C_{p,m}(\text{H}_2\text{O}) = (75.32 \pm 0.01) \text{ J}\cdot\text{K}^{-1}\cdot\text{mol}^{-1}$ [2]. The uncertainty of the measurements of the heat capacities was evaluated based on previous measurements of benzoic acid and hexafluorobenzene [27]. The combined expanded uncertainty is dependent

on the sample size used in each independent experimental run and was found to be typically in the order of 0.2 %; for ferrocene the combined expanded uncertainty was estimated to be $U_c(C_{p,m}) = 0.3 \text{ J}\cdot\text{K}^{-1}\cdot\text{mol}^{-1}$.

3.4. Sublimation enthalpy measurements (University of Porto)

The enthalpy of sublimation was measured calorimetrically using a Calvet high temperature microcalorimeter (Setaram, HT1000D) and the technique proposed by Skinner and co-workers [28] for the sublimation of solid compounds. The apparatus as well as the measuring technique have been described by Santos et al. [29]. The microcalorimeter was calibrated in situ for these measurements using the enthalpy of sublimation of naphthalene [15]. In a typical experiment, the solid sample, with a mass of 4 to 6 mg, was placed into a small glass capillary tube sealed at one end and weighed with a precision of 1 μg on an analytical balance. The sample tube and an empty reference tube were simultaneously dropped at room temperature into the hot reaction vessel and held at the working temperature of the calorimeter. An endothermic peak due to the heating of the sample from room temperature to the working temperature was first observed. When the signal returned to the baseline, the sample and reference cells were simultaneously evacuated, and the heat flow corresponding to the sublimation of the compound was measured. The thermal corrections for the glass tubes were determined in separate experiments, and those corrections were minimized by using tubes of nearly equal mass.

3.5. Phase behavior measurements (ICT Prague)

The phase behavior from 183 K to 473 K was investigated with a differential scanning calorimeter (TA Q1000, TA Instruments, USA) using the continuous method with heating rates of 2, 5, and 10 $\text{K}\cdot\text{min}^{-1}$. The two sample loads of 4.53 mg and 12.53 mg were determined by an analytical balance that had a readability of 0.01 mg and was periodically calibrated.

Prior to the measurements with ferrocene, a thorough temperature and enthalpy calibration was performed using water, gallium, naphthalene, indium, and tin at all of the heating rates used in this work. The crystal structure at 298.15 K was determined by x-ray diffraction (X'Pert PRO diffractometer, PANalytical, The Netherlands).

4. Results and discussion

4.1. Vapor pressures. The experimental vapor pressures obtained in this work are given in table 2. The literature data listed in table 3 were first critically assessed using the arc representation [30] (figure 1), which allowed us to reject obvious outliers. Afterwards, the consistency of the vapor pressure data with ideal gas heat capacities and heat capacities of condensed phases was tested. The selected vapor pressure data used in the SimCor method are given in bold in table 3.

4.2. Heat capacity of crystalline phase. The experimental heat capacities of the crystalline phase obtained in this work are listed in table 4; the literature data on heat capacities of crystalline phase are summarized in table 5. The selected heat capacity data used in the SimCor method are given in bold in table 5, and in the temperature range from 250 to 355 K they can be represented by a linear equation

$$C_{p,m}^{cr} / R = 8.04500 \cdot 10^{-2} (T / K) + 1.18541 \quad (6)$$

The heat capacities obtained in this work are compared with the literature values in figure 2. The data reported by Edwards and Kington [31] deviate by (0.02 to 0.04) $C_{p,m}^{cr} / R$ from equation (6), and the data by Joens and Gjaldbaek [32] and by Tomassetti et al. [33] deviate by approximately 0.015 $C_{p,m}^{cr} / R$. The uncertainty in the heat capacity of the crystalline phase affects the adjustment of sublimation enthalpy to the reference temperature as well as the calculation of the entropy of the crystal that is subsequently used to calculate the gaseous

entropy (the third-law entropy). The heat capacity data in these three publications were used by many researchers to adjust the sublimation enthalpy [34-39]. The entropy of the crystal reported by Edwards and Kington [31] was also used to calculate the third-law entropy, which was compared with the value obtained from spectroscopic data in attempts to estimate the energy barrier to internal rotation of cyclopentadienyl rings [31, 40]. We also note that Edwards and Kington [31] did not detect the orthorhombic crystal modification and consequently the phase transition from the orthorhombic to the monoclinic at 242 K, which has an entropy change of $(17.13 \pm 0.02) \text{ J}\cdot\text{K}^{-1}\cdot\text{mol}^{-1}$. Therefore, all calculations based on data [31-33] should be reconsidered.

4.3. Calorimetrically determined sublimation enthalpies.

Calorimetrically determined sublimation enthalpies obtained in this work are given in table 6, and the literature values are summarized in table 7. The results obtained here for the enthalpies of sublimation are in excellent agreement with the direct calorimetric results as well as with those derived indirectly from the temperature dependence of pressure reported in the literature. Indirect measurements of enthalpies of sublimation are more sensitive to the presence of volatile impurities than direct calorimetric methods. The uncertainty of the latter is more sensitive to the uncertainties of the method (heat flow measurement, calibration, temperature, sublimation speed) and less sensitive to the purity of sample. In the present work, the overall uncertainty was largely affected by the experimental temperature, which significantly affected the speed of sublimation and the total heat involved (heat capacity plus heat of sublimation). The calorimetric results clearly indicate that the enthalpy of sublimation decreases with increasing temperature. However, due to their short temperature interval (351.9 to 380.7 K) and their relatively larger uncertainty, the calorimetrically determined enthalpies did not play a significant role in the SimCor method.

4.4. Phase behavior.

Ferrocene is polymorphic [41, 42], with three crystal structures: monoclinic (stable above 242 K, metastable from 164 to 242 K), triclinic (metastable below 164 K), and orthorhombic (stable below 242 K). The crystal structure at 298.15 K was determined in this work using x-ray diffraction as monoclinic, space group $P2_1/a$, with $a = 10.539 \text{ \AA}$, $b = 7.612 \text{ \AA}$, $c = 5.933 \text{ \AA}$, and $\beta = 121.05^\circ$. No crystal phase transition was detected during our differential scanning calorimeter (DSC) studies in the temperature range from 183 K to the temperature of fusion, even after the sample was annealed at 183 K for several hours. This agrees with literature findings that the monoclinic crystal structure supercools readily and that it is difficult to obtain the orthorhombic structure [41], which was not detected before 1979 [43, 44]. We conclude that all of the present measurements were performed with the monoclinic structure.

We measured the temperature of fusion T_{fus} and enthalpy of fusion $\Delta_{\text{cr}}^{\ell}H_{\text{m}}$ 24 times using sample masses of 12.55 and 4.55 mg and heating rates of 2, 5, and 10 K min⁻¹. The individual values (see table S1 in the supporting information) had no dependence on mass and heating rate, and the mean values were $T_{\text{fus}} = (446.9 \pm 0.3) \text{ K}$ and $\Delta_{\text{cr}}^{\ell}H_{\text{m}} = (18.1 \pm 0.3) \text{ kJ mol}^{-1}$. The expanded uncertainties quoted are twice the standard deviation of the mean. The temperature of fusion was characterized as the onset temperature of the fusion peak; the enthalpy of fusion was determined by integration of the fusion peak using a linear baseline. As T_{fus} did not shift to a lower value after multiple heatings to 473.15 K, it can be concluded that ferrocene is thermally stable up to this temperature. Table 8 compares the present values of T_{fus} and $\Delta_{\text{cr}}^{\ell}H_{\text{m}}$ with literature values. Most publications used DSC except [45] (differential thermal analysis), [32] (drop calorimetry along with heat capacity [31]), and [46] [47] (measuring technique not mentioned), and therefore they should have similar uncertainties. We assumed that the temperature and enthalpy calibrations were properly performed, although the calibration was often not described in the DSC papers. The mean value was calculated from the data that are in mutual agreement and where the measuring technique is well documented;

these data are given in bold in table 8. The mean values so obtained are $T_{\text{fus}} = (447.3 \pm 1.3) \text{ K}$ and $\Delta_{\text{cr}}^{\ell} H_{\text{m}} = (17.9 \pm 0.3) \text{ kJ}\cdot\text{mol}^{-1}$ ($k = 2$).

4.5. Thermodynamic properties in the ideal gas state.

The thermodynamic properties in the ideal gas state were calculated by statistical mechanics using the rigid rotor – harmonic oscillator (RRHO) approximation with correction for internal rotations. Molecular geometry optimizations and vibrational frequencies calculations were performed using the density functional theory (DFT) at the B3LYP/6-311+G(2df,p) level of theory with the Gaussian 03 software package [48]. The molecular structure obtained by optimization at this level corresponds to the eclipsed conformation (symmetry point group D_{5h} , external symmetry number $\sigma = 10$, see figure 3), and it is in good agreement with that of the free molecule determined experimentally by gas-phase electron diffraction [4] and that calculated by the higher level *ab initio* method of coupled-cluster singles-and-doubles with a perturbative triples correction (CCSD(T)) [49]. This confirms that DFT with the B3LYP functional accurately predicts the molecular structure of ferrocene. The principal moments of inertia used to calculate the contributions of the general rotation were $I_{\text{A}} = 3.795 \cdot 10^{-45} \text{ kg}\cdot\text{m}^2$, $I_{\text{B}} = I_{\text{C}} = 8.055 \cdot 10^{-45} \text{ kg}\cdot\text{m}^2$, and the molar mass used to calculate the translation contribution was $M = 186.03 \text{ g}\cdot\text{mol}^{-1}$.

The calculated vibrational frequencies were scaled by 0.9767 (wavenumbers $< 2000 \text{ cm}^{-1}$) and 0.9629 (wavenumbers $> 2000 \text{ cm}^{-1}$). These general scale factors were obtained recently by comparing calculations for 93 rigid molecules with reliable reference data [50]. We calculated the vibrational contribution to thermodynamic properties with both scaled calculated frequencies and experimental frequencies [51] (note that other experimental spectra, for example [46, 52], are incomplete), but we consider the former to be more reliable due to the following reasons: i) Experimental frequencies were obtained for crystalline ferrocene in which the molecules are not isolated but interact with each other. The resulting lower point

symmetry of the molecule causes the normal frequencies to differ somewhat from those of the molecule with D_{5h} symmetry [52, 53]. The low-frequency modes, whose accuracy is crucial for the calculation of the ideal-gas thermodynamic properties, are the most affected. ii) The assignments of the vibrational modes that were originally suggested by Lippincott and Nelson [46] and the accuracy of the experimental determinations still have ambiguities [52-56]. iii) The ideal-gas thermodynamic properties obtained using the calculated frequencies show a better consistency with vapor pressures.

The contributions of internal rotations of cyclopentadienyl rings were calculated using the one-dimensional hindered rotor (1-D HR) scheme [57], which requires the barrier to internal rotation, the reduced moment of inertia I_r for internal rotation, the internal symmetry number ($\sigma_{\text{int}} = 5$), and the identification and exclusion of the torsional mode from the vibrational contribution to the partition function. The DFT calculation yielded a value for the barrier to internal rotation ΔE (the energy difference between the staggered (D_{5d}) and eclipsed (D_{5h}) conformations, see figure 3) that had only moderate accuracy because it depended strongly on the basis set. The calculations performed with the second order Møller–Plesset perturbation theory (MP2) showed a significant overestimation of the barrier energy. Therefore, we employed the experimental value determined by Bohn and Haaland [4], $\Delta E = (3.77 \pm 1.26)$ $\text{kJ}\cdot\text{mol}^{-1}$, which is in accordance with a recent CCSD(T) calculation [49]. The reduced moment of inertia I_r for internal rotation was calculated according to Pitzer [58] from the optimized geometrical parameters of the molecule, $I_r = 1.467 \cdot 10^{-45}$ $\text{kg}\cdot\text{m}^2$. The energy levels were obtained by solving a one-dimensional Schrödinger equation for hindered internal rotation using the program *StatTD* [59].

Table 9 lists the ideal-gas thermodynamic properties obtained using the 1-D HR scheme and scaled B3LYP/6-311+G(2df,p) frequencies, and figure 4 compares them with the literature values and with the present calculations based on experimental frequencies [51]. Many authors reporting vapor pressure and sublimation enthalpy measurements, for example [29,

35-39, 60], used ideal-gas heat capacity data by Turnbull [61] or Lippincott and Nelson [62] for the adjustment of sublimation enthalpy to the reference temperature. Therefore, we find it useful to compare our calculations with these two datasets. The ideal-gas thermodynamic data reported by Lippincott and Nelson [62] (calculated using structural parameters and vibrational frequencies available at that time [46, 63] and assuming free rotation of cyclopentadienyl rings) are in reasonable agreement, while the subsequent data reported by Turnbull [61] (calculated using structural parameters [4] and vibrational frequencies [64] and assuming restricted internal rotation with the energy barrier of $4.6 \text{ kJ}\cdot\text{mol}^{-1}$) are in disagreement with our calculations and other literature data [65]. This suggests that the enthalpy adjustments calculated using the data by Turnbull [61] should be reconsidered.

4.6. Recommended vapor pressure data developed by the SimCor method

The SimCor method was used to correlate simultaneously the selected vapor pressure data (bold in table 3), the selected heat capacities of the crystalline phase (bold in table 5), and the calculated ideal gas heat capacities (table 9). The pVT properties used in equations (1) and (2) were evaluated from the virial equation of state with the second virial coefficient estimated by the method of Tsonopoulos [66]. This method requires critical temperature T_c , critical pressure p_c , and acentric factor ω . Ferrocene decomposes well below critical temperature, but Nikitin and Popov [67] succeeded to measure critical parameters by using pulse-heating method. Nikitin and Popov published also value of acentric factor based on vapor pressures by Nisel'son et al. [68] and by Barkatin et al. [69]. As enthalpies of vaporization derived from Barkatin et. al. data are obviously unreliable, we redetermined acentric factor in the following way. The simultaneous correlation of vapor pressure data for liquid ferrocene reported by Nisel'son et al. [68], those obtained in this work (3 points in table 2), and the vaporization enthalpy at T_{tp} derived from $\Delta_{cr}^g H_m(T_{tp})$ and $\Delta_{cr}^l H_m(T_{tp})$ led to the following parameters of the Cox equation (3) for the liquid phase: $A_0 = 2.632489$, $A_1 = 3.357441\cdot 10^{-4}$, $A_2 = -7.568057\cdot 10^{-7}$, $T_0 = 473.3 \text{ K}$, and $p_0 = 16750 \text{ Pa}$. Using these parameters acentric factor $\omega =$

0.258 was calculated. Note that the uncertainty of these parameters cannot be quantified because Nisel'son et al. did not report their measurement uncertainties and their data cannot be compared with other datasets in the given temperature range. Therefore, the above parameters for the liquid phase should be used with caution.

Given the uncertainty of T_c , p_c and ω , the heat capacity data spanned only the temperature range in which the uncertainty of the pVT data was negligible in the process of simultaneous correlation of solid phase properties. Even a significant change of critical parameters had a negligible impact on the SimCor results. The molar volume of the crystalline phase along the saturation line also has negligible role in this temperature range and was therefore neglected.

The recommended values of vapor pressure for crystalline ferrocene are represented by the Cox equation (4) using the parameters given in table 10. Recommended vapor pressures and sublimation enthalpies obtained by using the Clapeyron equation are listed at rounded temperatures in table 11. The reported uncertainties reflect the uncertainties in the selected input data for the SimCor method and the uncertainty in the equation of state. Figure 5 shows the deviations of the literature values from our recommended values, and figure 6 shows the corresponding deviations for the enthalpy of sublimation. Our value of sublimation enthalpy $\Delta_{cr}^g H_m(298.15\text{ K}) = (74.38 \pm 0.38) \text{ kJ}\cdot\text{mol}^{-1}$ agrees with the ICTAC value $\Delta_{cr}^g H_m(298.15\text{ K}) = (73.42 \pm 1.08) \text{ kJ}\cdot\text{mol}^{-1}$ [2], but it has a smaller uncertainty. Figure 7 demonstrates a good consistency between the difference in the heat capacities of the gaseous and crystalline phases and the difference calculated from the recommended vapor pressure data.

5. Conclusions

A recommended vapor pressure equation and thermophysical property data for ferrocene were developed by a multi-property fit to selected experimental vapor pressure data and the differences in heat capacities of crystalline phase and ideal gas. New experimental data on the vapor pressure, enthalpies of sublimation, and heat capacity of crystalline phase were

determined in this work. The thermodynamic properties in the ideal gaseous state were calculated by the methods of statistical thermodynamics in combination with the DFT B3LYP/6-311+G(2df,p) frequencies and 1-D HR formalism for the treatment of internal rotations.

Acknowledgements

We thank Vladimir Diky and Ala Bazyleva for providing the program *StatTD*. This work was supported by the Ministry of Education of the Czech Republic under project ME10049, the Czech Science Foundation under project 203/09/1327, and the NIST Office of Microelectronic Programs. Marisa A. A. Rocha acknowledges the financial support from FCT and the European Social Fund (ESF) under the Community Support Framework (CSF) for the award of a Research Grants SFRH/BD/60513/2009.

Supplementary data

Supplementary data associated with this article can be found, in the online version, at doi .

References

- [1] A.C.G. van Genderen, H.A.J. Oonk, *Colloid Surf. A-Physicochem. Eng. Asp.* 213 (2003) 107-115.
- [2] R. Sabbah, X.W. An, J.S. Chickos, M.L.P. Leitao, M.V. Roux, L.A. Torres, *Thermochim. Acta* 331 (1999) 93-204.
- [3] J.S. Chickos, D.G. Hesse, J.F. Liebman, *Struct. Chem.* 4 (1993) 261-269.
- [4] R.K. Bohn, A. Haaland, *J. Organomet. Chem.* 5 (1966) 470-476.
- [5] K. Růžička, V. Majer, *Fluid Phase Equilib.* 28 (1986) 253-264.
- [6] K. Růžička, V. Majer, *J. Phys. Chem. Ref. Data* 23 (1994) 1-39.

- [7] K. Růžička, V. Majer, *AIChE J.* 42 (1996) 1723-1740.
- [8] E.R. Cox, *Ind. Eng. Chem.* 15 (1923) 592-593.
- [9] V. Roháč, V. Růžička, K. Růžička, M. Poledníček, K. Aim, J. Jose, M. Zábranský, *Fluid Phase Equilib.* 157 (1999) 121-142.
- [10] V. Roháč, J.E. Musgrove, K. Růžička, V. Růžička, M. Zábranský, K. Aim, *J. Chem. Thermodyn.* 31 (1999) 971-986.
- [11] K. Růžička, I. Mokbel, V. Majer, V. Růžička, J. Jose, M. Zábranský, *Fluid Phase Equilib.* 148 (1998) 107-137.
- [12] I. Mokbel, K. Růžička, V. Majer, V. Růžička, M. Ribeiro, J. Jose, M. Zábranský, *Fluid Phase Equilib.* 169 (2000) 191-207.
- [13] V. Růžička, M. Zábranský, K. Růžička, V. Majer, *Thermochim. Acta* 245 (1994) 121-144.
- [14] V. Roháč, K. Růžička, V. Růžička, D.H. Zaitsau, G.J. Kabo, V. Diky, K. Aim, *J. Chem. Thermodyn.* 36 (2004) 929-937.
- [15] K. Růžička, M. Fulem, V. Růžička, *J. Chem. Eng. Data* 50 (2005) 1956-1970.
- [16] M. Fulem, K. Růžička, V. Růžička, T. Šimeček, E. Hulicius, J. Pangrác, *J. Chem. Thermodyn.* 38 (2006) 312-322.
- [17] M. Fulem, K. Růžička, M. Růžička, *Fluid Phase Equilib.* 303 (2011) 205-216.
- [18] M. Fulem, K. Růžička, P. Morávek, J. Pangrác, E. Hulicius, B. Kozyrkin, V. Shatunov, *J. Chem. Eng. Data* 55 (2010) 4780–4784.
- [19] Certain commercial equipment, or materials are identified in this paper in order to specify the experimental procedure adequately. Such identification is not intended to imply recommendation or endorsement by the National Institute of Standards and Technology, nor is it intended to imply that the materials or equipment identified are necessarily the best available for the purpose.

- [20] R.F. Berg, *Journal of the National Institute of Standards and Technology* (in preparation, 2012).
- [21] R.F. Berg, *Rev. Sci. Instrum.* 82 (2011) 085110 -085115.
- [22] G.W.H. Höhne, W.F. Hemminger, H.-J. Flammersheim, *Differential Scanning Calorimetry*, 2 ed., Springer Verlag, Berlin, 2003.
- [23] M. Straka, K. Růžička, V. Růžička, *J. Chem. Eng. Data* 52 (2007) 1375-1380.
- [24] M. Fulem, V. Laštovka, M. Straka, K. Růžička, J.M. Shaw, *J. Chem. Eng. Data* 53 (2008) 2175-2181.
- [25] J. Koníček, I. Wadsö, J. Suurkuus, *Chem. Scr.* 1 (1971) 217-220.
- [26] J. Suurkuus, I. Wadsö, *J. Chem. Thermodyn.* 6 (1974) 667-679.
- [27] L.M.N.B.F. Santos, M.A.A. Rocha, A.S.M.C. Rodrigues, V. Štejfa, M. Fulem, M. Bastos, *J. Chem. Thermodyn.* 43 (2011) 1818-1823.
- [28] F.A. Adedeji, D.L.S. Brown, J.A. Connor, M.L. Leung, I.M. Pazandrade, H.A. Skinner, *J. Organomet. Chem.* 97 (1975) 221-228.
- [29] L.M.N.B.F. Santos, B. Schröder, O.O.P. Fernandes, M.A.V. Ribeiro da Silva, *Thermochim. Acta* 415 (2004) 15-20.
- [30] M. Čenský, V. Roháč, K. Růžička, M. Fulem, K. Aim, *Fluid Phase Equilib.* 298 (2010) 192-198.
- [31] J.W. Edwards, G.L. Kington, *T. Faraday Soc.* 58 (1962) 1334-1340.
- [32] O. Joens, J.C. Gjaldbaek, *Dan. Tidsskr. Farm.* 43 (1969) 151-155.
- [33] M. Tomassetti, R. Curini, G. D'Ascenzo, G. Ortaggi, *Thermochim. Acta* 48 (1981) 333-341.
- [34] M.A.V. Ribeiro da Silva, M.J.S. Monte, *Thermochim. Acta* 171 (1990) 169-183.
- [35] M. Pelino, M. Tomassetti, V. Piacente, G. D'Ascenzo, *Thermochim. Acta* 44 (1981) 89-99.

- [36] L.A. Torres, R. Gudino, R. Sabbah, J.A. Guardado, *J. Chem. Thermodyn.* 27 (1995) 1261-1266.
- [37] A. Rojas-Aguilar, E. Orozco-Guareño, M. Martínez-Herrera, *J. Chem. Thermodyn.* 33 (2001) 1405-1418.
- [38] T. Kiyobayashi, M.E. M. da Piedade, *J. Chem. Thermodyn.* 33 (2001) 11-21.
- [39] C.M. Lousada, S.S. Pinto, J.N.C. Lopes, M.F.M. da Piedade, H.P. Diogo, M.E.M. da Piedade, *J. Phys. Chem. A* 112 (2008) 2977-2987.
- [40] J.T.S. Andrews, E.F. Westrum, *J. Organomet. Chem.* 17 (1969) 349-352.
- [41] J.D. Dunitz, *Acta Crystallogr., Sect. B: Struct. Sci.* 51 (1995) 619-631.
- [42] K. Ogasahara, M. Sorai, H. Suga, *Mol. Cryst. Liq. Cryst.* 71 (1981) 189-211.
- [43] K. Ogasahara, M. Sorai, H. Suga, *Chem. Phys. Lett.* 68 (1979) 457-460.
- [44] J.-F. Bérar, G. Calvarin, D. Weigel, K. Chhor, C. Pommier, *The Journal of Chemical Physics* 73 (1980) 438-441.
- [45] R. Sabbah, J.A.G. Perez, *Thermochim. Acta* 297 (1997) 17-32.
- [46] E.R. Lippincott, R.D. Nelson, *Spectrochimica Acta* 10 (1958) 307-329.
- [47] J.W. Edwards, G.L. Kington, R. Mason, *T. Faraday Soc.* 56 (1960) 660-667.
- [48] M.J. Frisch, G.W. Trucks, H.B. Schlegel, G.E. Scuseria, M.A. Robb, J.R. Cheeseman, J. Montgomery, J. A., T. Vreven, K.N. Kudin, J.C. Burant, J.M. Millam, S.S. Iyengar, J. Tomasi, V. Barone, B. Mennucci, M. Cossi, G. Scalmani, N. Rega, G.A. Petersson, H. Nakatsuji, M. Hada, M. Ehara, K. Toyota, R. Fukuda, J. Hasegawa, M. Ishida, T. Nakajima, Y. Honda, O. Kitao, H. Nakai, M. Klene, X. Li, J.E. Knox, H.P. Hratchian, J.B. Cross, V. Bakken, C. Adamo, J. Jaramillo, R. Gomperts, R.E. Stratmann, O. Yazyev, A.J. Austin, R. Cammi, C. Pomelli, J.W. Ochterski, P.Y. Ayala, K. Morokuma, G.A. Voth, P. Salvador, J.J. Dannenberg, V.G. Zakrzewski, S. Dapprich, A.D. Daniels, M.C. Strain, O. Farkas, D.K. Malick, A.D. Rabuck, K. Raghavachari, J.B. Foresman, J.V. Ortiz, Q. Cui, A.G. Baboul, S. Clifford, J. Cioslowski, B.B. Stefanov, G. Liu, A. Liashenko, P. Piskorz, I. Komaromi, R.L.

Martin, D.J. Fox, T. Keith, M.A. Al-Laham, C.Y. Peng, A. Nanayakkara, M. Challacombe, P.M.W. Gill, B. Johnson, W. Chen, M.W. Wong, C. Gonzalez, J.A. Pople, Gaussian, Inc., Wallingford CT, 2004.

- [49] S. Coriani, A. Haaland, T. Helgaker, P. Jorgensen, *ChemPhysChem* 7 (2006) 245-249.
- [50] C. Červinka, M. Fulem, K. Růžička, *J. Chem. Eng. Data* 57 (2012) 227-232.
- [51] J.S. Bodenheimer, W. Low, *Spectrochim. Acta, Part A* 29 (1973) 1733-1743.
- [52] E. Kemner, I.M. de Schepper, G.J. Kearley, U.A. Jayasooriya, *J. Chem. Phys.* 112 (2000) 10926-10929.
- [53] A. Bérces, T. Ziegler, L. Fan, *J. Phys. Chem.* 98 (1994) 1584-1595.
- [54] Z.-F. Xu, Y. Xie, W.-L. Feng, H.F. Schaefer, *J. Phys. Chem. A* 107 (2003) 2716-2729.
- [55] Y.M. Kimel'fel'd, E.M. Smirnova, V.T. Aleksanyan, *J. Mol. Struct.* 19 (1973) 329-346.
- [56] B.V. Lokshin, V.T. Aleksanian, E.B. Rusach, *J. Organomet. Chem.* 86 (1975) 253-256.
- [57] J. Pfaendtner, X. Yu, L.J. Broadbelt, *Theoretical Chemistry Accounts* 118 (2007) 881-898.
- [58] K.S. Pitzer, W.D. Gwinn, *J. Chem. Phys.* 10 (1942) 428-440.
- [59] V. Diky, A. Bazyleva, private communication, 2011.
- [60] M.A.V.R. Da Silva, M.J.S. Monte, *Thermochim. Acta* 171 (1990) 169-183.
- [61] A.G. Turnbull, *Aust. J. Chem.* 20 (1967) 2059-2067.
- [62] E.R. Lippincott, R.D. Nelson, *J. Am. Chem. Soc.* 77 (1955) 4990-4993.
- [63] P.F. Eiland, R. Pepinsky, *J. Am. Chem. Soc.* 74 (1952) 4971-4971.
- [64] H.P. Fritz, *Adv. Organomet. Chem.* 1 (1964) 239-316.
- [65] A. Rojas, M.T. Vieyra-Eusebio, *J. Chem. Thermodyn.* 43 (2011) 1738-1747.
- [66] C. Tsionopoulos, *AIChE J.* 20 (1974) 263-272.
- [67] E.D. Nikitin, A.P. Popov, *Fluid Phase Equilib.* 324 (2012) 13-16.

- [68] L.A. Nisel'son, T.D. Sokolova, R.K. Nikolaev, Vestnik Moskovskogo Universiteta, Seriya 2: Khimiya 13 (1972) 432-434.
- [69] A.A. Barkatin, I.L. Gaidym, A.K. Baev, Khim. Khim. Tekhnol. (Minsk) 12 (1977) 44-48.
- [70] L. Kaplan, W.L. Kester, J.J. Katz, J. Am. Chem. Soc. 74 (1952) 5531-5532.
- [71] J.F. Cordes, S. Schreiner, Z Anorg Allg Chem 299 (1959) 87-91.
- [72] J.W. Edwards, G.L. Kington, T. Faraday Soc. 58 (1962) 1323-1333.
- [73] J.C.G. Calado, A.R. Dias, M.E. Minas da Piedade, J.A.M. Simoes, Rev. Port. Quim. 22 (1980) 53-58.
- [74] J. Sachinidis, J.O. Hill, Thermochim. Acta 35 (1980) 59-66.
- [75] M.H.G. Jacobs, P.J. van Ekeren, C.G. de Kruif, J. Chem. Thermodyn. 15 (1983) 619-623.
- [76] L.A. Torres-Gómez, G. Barreiro-Rodríguez, F. Méndez-Ruíz, Thermochim. Acta 124 (1988) 179-183.
- [77] M.J.S. Monte, L.M.N.B.F. Santos, M. Fulem, J.M.S. Fonseca, C.A.D. Sousa, J. Chem. Eng. Data 51 (2006) 757-766.
- [78] M.A. Siddiqi, B. Atakan, Thermochim. Acta 452 (2007) 128-134.
- [79] V.N. Emel'yanenko, S.P. Verevkin, O.V. Krol, R.M. Varushchenko, N.V. Chelovskaya, J. Chem. Thermodyn. 39 (2007) 594-601.
- [80] G. Beech, R.M. Lintonbon, Thermochim. Acta 2 (1971) 86-88.
- [81] J.P. Murray, K.J. Cavell, J.O. Hill, Thermochim. Acta 36 (1980) 97-101.
- [82] M. Dabrowski, B. Misterkiewicz, A. Sporzyński, J. Chem. Eng. Data 46 (2001) 1627-1631.

TABLE 1

Sample description.

Chemical Name	CAS Registry Number	Source	Initial Mole Fraction Purity	Purification Method	Final Mole Fraction Purity	Analysis Method
ferrocene	102-54-5	Aldrich	0.998	vacuum sublimation	0.9998 ^a	GC ^b

^a Result of the two independent GC analyses performed at the University of Porto and

Institute of Chemical Technology Prague

^b Gas-liquid chromatography (chromatographs HP 4890 and 6890 were employed)

TABLE 2Experimental vapor pressures p .

T / K	p / Pa	T / K	p / Pa	T / K	p / Pa	T / K	p / Pa
ICT Prague ^{a,b}				NIST ^c			
288.16	0.360	300.17	1.191	322.209	9.00	362.171	185.06
288.16	0.355	300.17	1.195	322.212	9.11	362.178	184.76
288.16	0.353	301.17	1.316	332.202	20.78	362.184	185.47
289.18	0.387	301.17	1.315	332.208	20.86	372.197	354.19
289.18	0.386	302.18	1.425	332.211	20.71	382.169	648.18
289.18	0.386	302.18	1.424	342.163	44.33	382.193	651.13
290.17	0.426	302.18	1.403	342.170	44.39	392.198	1157.6
290.17	0.425	303.18	1.611	342.178	44.97	402.247	2006.2
290.17	0.423	303.18	1.601	342.179	45.17	402.249	2005.2
291.17	0.469	303.18	1.605	352.166	92.62	402.264	2000.5
291.17	0.472	304.18	1.759	352.168	92.80	402.277	2001.2
291.17	0.474	304.18	1.762	352.169	93.25	402.311	2008.1
292.16	0.547	304.18	1.752	352.169	92.72	412.238	3345.9
292.16	0.538	305.18	1.937	352.171	93.73	412.318	3360.6
292.16	0.541	305.18	1.940	352.172	93.40	422.287	5470.1
293.16	0.588	305.18	1.939	352.176	92.49	422.403	5501.7
293.16	0.592	306.18	2.128	352.176	92.64	432.418	8756.2
293.16	0.585	306.18	2.128	352.182	93.28	442.265	13532
294.16	0.668	306.18	2.136	352.192	93.60	451.844 ^d	19481 ^d
294.16	0.665	307.18	2.347	362.164	184.76	451.954 ^d	19212 ^d
294.16	0.651	307.18	2.350	362.170	185.00	452.085 ^d	19481 ^d
295.17	0.711	307.18	2.349				
295.17	0.707	308.18	2.581				
295.17	0.695	308.18	2.572				
296.17	0.802	308.18	2.587				
296.17	0.803	309.18	2.804				
296.17	0.803	309.18	2.788				
297.17	0.876	309.18	2.806				
297.17	0.878	310.18	3.109				
298.17	0.980	310.18	3.104				
298.17	0.985	310.18	3.108				
298.17	0.980	311.19	3.412				
299.18	1.083	311.19	3.412				
299.18	1.089	311.19	3.400				
300.17	1.200						

^a Standard uncertainties u are $u(T) = 0.02 \text{ K}$ and $u(p) = 0.005 p + 0.05 \text{ Pa}$.^b Values are reported with one digit more than is justified by the experimental uncertainty to avoid round-off errors in calculations based on these results.^c Standard uncertainties u are $u(T) = 0.012 \text{ K}$ and $u(p < 1 \text{ kPa}) = 0.0014 p + 0.01 \text{ Pa}$ and $u(p > 1 \text{ kPa}) = 0.0001 p + 1 \text{ Pa}$

^d Liquid phase.

TABLE 3Overview of the literature vapor pressure data.^a

Reference	N^b	$(T_{\min}-T_{\max}) /$ K	$(p_{\min}-p_{\max}) /$ kPa	$u(T)^c /$ K	$u(p)^d /$ Pa	Purity ^e	Method
Kaplan et al. [70]	S ^g	357-456	0.123-21.251	-	-	-	Static
Kaplan et al. [70] ^f	S	456-556	21.251-198.909	-	-	-	Static
Cordes and Schreiner [71]	5	324-367	0.011-0.288	-	0.05 p	-	ME ^h
Edwards and Kington [72]	25	295-303	$6.9 \cdot 10^{-4}$ - $1.6 \cdot 10^{-3}$	-	-	-	ME
Andrews and Westrum [40]	7	294-306	$6.4 \cdot 10^{-4}$ - $2.0 \cdot 10^{-3}$	-	-	-	ME
Nisel'son et al. [68] ^f	13	518-604	106.1-483.4	-	-	-	Ebulliometry
Barkatin et al. [69]	S	348-451	0.103-17.019	-	-	-	Static
Barkatin et al. [69] _f	S	451-523	17.807-110.351	-	-	-	Static
Calado et al. [73]	16	297-301	$8.4 \cdot 10^{-4}$ - $1.2 \cdot 10^{-3}$	-	-	-	ME
Sachinidis and Hill [74]	1	336	$2.4 \cdot 10^{-3}$	0.05	5	-	Static
Pelino et al. [35]	46	288-353	$5.7 \cdot 10^{-4}$ -0.090	-	-	-	TE ⁱ
Jacobs et al. [75]	S	277-297	$9.8 \cdot 10^{-5}$ - $1.0 \cdot 10^{-3}$	-	-	>0.99	TE
Jacobs et al. [75]	S	277-297	$1 \cdot 10^{-4}$ - $9.9 \cdot 10^{-4}$	-	-	>0.99	ME
Jacobs et al. [75]	9	329-360	0.018-0.166	-	-	>0.99	Static
Torres-Gómez et al. [76]	10	278-309	$1.3 \cdot 10^{-4}$ - $2.9 \cdot 10^{-3}$	-	-	0.999	ME
Da Silva and Monte [60]	48	292-300	$5.6 \cdot 10^{-4}$ - $1.3 \cdot 10^{-3}$	0.01	-	-	ME
Monte et al. [77]	54	288-356	$3.6 \cdot 10^{-4}$-0.121	0.01	$1 \cdot 10^{-5}$ +0.0025 p	0.9999	Static
Siddiqi and Atakan [78]	S	295.00-325.00	$7.9 \cdot 10^{-4}$ -0.012	0.1	0.02 to 0.5 Pa ^j	>0.99	ME
Emel'yanenko et al. [79]	18	289.70-363.40	$4.1 \cdot 10^{-4}$ -0.180	0.1	-	>0.998	Transpiration
Lousada et al. [39]	9	298-304	$8.8 \cdot 10^{-4}$ - $1.5 \cdot 10^{-3}$	0.01	-	>0.98	ME
This work	108	288-442	$3.6 \cdot 10^{-4}$ – 13.532	table 2	table 2	0.9998	static

^a The data from references written in bold were used in the SimCor method.

^b N = number of experimental points.

^c $u(T)$ = uncertainty in temperature when reported by the authors.

^d $u(p)$ = uncertainty in pressure when reported by the authors.

^e Mole fraction purity indicated if available.

^f Liquid phase.

^g S = smoothed data.

^h ME = mass-loss effusion.

ⁱ TE = torsion effusion.

^j Uncertainty in pressure depends on the pressure.

TABLE 4Experimental molar heat capacities of the crystalline phase $C_{p,m}^{\text{cr}}$.

T / K	$C_{p,m}^{\text{cr}} / (\text{J}\cdot\text{K}^{-1}\cdot\text{mol}^{-1})$
ICT Prague ^{a,b}	
273.40	172.6
278.52	177.0
283.62	180.4
288.72	183.8
293.83	186.2
298.93	189.9
304.04	194.0
309.14	197.2
314.25	200.6
319.35	204.4
324.46	207.0
329.56	211.3
334.66	214.2
339.77	218.0
344.88	220.2
349.98	223.7
355.09	227.2
University of Porto ^{c,d}	
298.15	189.4

^a The standard uncertainty of the temperature is $u(T) = 0.05 \text{ K}$, and the combined expanded uncertainty of the heat capacity is $U_c(C_{p,m}^{\text{cr}}) = 0.01 C_{p,m}^{\text{cr}}$ (0.95 level of confidence).

^b Calvet calorimeter. Mean values of the duplicate experiments.

^c Standard uncertainty of the temperature is $u(T) = 0.01 \text{ K}$, and the combined expanded uncertainty of the heat capacity is $U_c(C_{p,m}^{\text{cr}}) = 0.3 \text{ J K}^{-1} \text{ mol}^{-1}$ (0.95 level of confidence).

^d Drop calorimeter. Mean value of five determinations.

TABLE 5Overview of the literature heat capacities of crystalline phase.^a

Reference	$(T_{\min}-T_{\max})/K$	$u(C_p)^b$	Purity ^c	Method
Edwards and Kington [31]	17-300	0.002 C_p	-	AC ^d
Joens and Gjaldbaek [32]	405-445	0.03 C_p	-	DC ^e
Tomassetti et al. [33]	293-393	2.1 J·K ⁻¹ ·mol ⁻¹	-	DSC ^f
Ogasahara et al. [42]	13-300	-	-	AC
Rojas et and Vieyra-Eusebio [65]	293-353	-	0.9991	DSC
This work	273-355	table 4	0.9998	CC^g and DC

^a The data from references written in bold were used in the development of equation (6) and in the SimCor method.

^b $u(C_p)$ = uncertainty in heat capacity reported by the authors.

^c Mole fraction purity indicated if available.

^d AC = adiabatic calorimetry.

^e DC = drop calorimetry.

^f DSC = differential scanning calorimetry.

^g CC = Calvet calorimetry.

TABLE 6

The total enthalpy change $\Delta_{\text{cr},298.15\text{K}}^{\text{g},T} H_{\text{m}}$, the applied molar enthalpic corrections for the heat capacity of the crystalline phase $H_{\text{m}}(\text{cr}, T) - H_{\text{m}}(\text{cr}, 298.15 \text{ K})$, and the molar sublimation enthalpies $\Delta_{\text{cr}}^{\text{g}} H_{\text{m}}$.^a

Experiment	T/K	$\Delta_{\text{cr},298.15\text{K}}^{\text{g},T} H_{\text{m}}$	$H_{\text{m}}(\text{cr}, T) - H_{\text{m}}(\text{cr}, 298.15 \text{ K})^{\text{b}}$	$\Delta_{\text{cr}}^{\text{g}} H_{\text{m}} / (\text{kJ} \cdot \text{mol}^{-1})$	$U_{\text{c}} (\Delta_{\text{cr}}^{\text{g}} H_{\text{m}}) / (\text{kJ} \cdot \text{mol}^{-1})^{\text{c}}$
1	380.7	87.7	17.9	69.8	0.8
2	362.6	83.9	13.6	70.3	0.6
3	351.9	83.6	11.2	72.4	0.4

^a Standard uncertainty of the temperature is $u(T) = 0.05 \text{ K}$

^b Calculated using heat capacity of the crystalline phase represented by equation (6).

^c Combined expanded uncertainty (0.95 level of confidence).

TABLE 7

Overview of the literature calorimetric enthalpies of sublimation.

Reference	N^a	$(T_{\min}-T_{\max}) /$ K	$\Delta_{\text{cr}}^{\text{g}} H_{\text{m}}(T) /$ (kJ·mol ⁻¹)	$(\Delta_{\text{cr}}^{\text{g}} H_{\text{m}, \min} -$ $\Delta_{\text{cr}}^{\text{g}} H_{\text{m}, \max})^b /$ (kJ·mol ⁻¹)	$u(\Delta_{\text{cr}}^{\text{g}} H_{\text{m}})^c /$ (kJ·mol ⁻¹)	Purity ^d	Method
Beech and Lintonbon [80]	1	385-455	84	-	2	-	DSC ^e
Murray et al. [81]	5		70	-	2	-	DSC
Torres et al. [36]	12	298	73.19	72.10-74.34	0.66	0.9999	CC ^f
Rojas-Aguilar et al. [37]	11	333	71.84	70.12-79.91	1.38	0.9997	DSC
Kiyobayashi et Minas da Piedade [38]	5	313	72.64	72.51-72.74	0.12	-	DCC ^g
Santos et al. [29]	6	373	71.8	70.83-73.76	1.0	-	DCC
Lousada et al. [39]	6	298	72.71	-	0.23	-	DCC
Rojas et and Vieyra-Eusebio [65]	14	333	72.2	70.4-73.7	1.2	0.9991	DSC
Rojas and Vieyra-Eusebio[65]	10	333	73.3	70.2-74.3	1.2	0.9991	CC
This work	3	352-381	-	69.8-72.4	table 6	0.9998	DCC

^a N = number of experimental points.^b For the measurements taken at single temperature the enthalpy range corresponds to the spread of the measured values.^c $u(\Delta_{\text{cr}}^{\text{g}} H_{\text{m}})$ = uncertainty in enthalpy measurement when reported by the authors.^d Mole fraction purity indicated if available.^e DSC = differential scanning calorimetry.^f CC = Calvet calorimetry.^g DCC = drop Calvet calorimetry.

TABLE 8

Comparison of temperature and enthalpy of fusion with the literature values.

Reference	Method	Purity ^a	$T_{\text{fus}} / \text{K}$	$\Delta_{\text{cr}}^{\ell} H_{\text{m}} / (\text{kJ} \cdot \text{mol}^{-1})$
Lippincott and Nelson [46]	-	-	446.2-447.2	-
Edwards et al. [47]	-	-	448.2-448.7	-
Joens and Gjaldbaek [32]	DC ^c	-	448.7	$17.8 \pm 0.4^{\text{b}}$
Beech and Lintonbon [80]	DSC ^d	-	-	$18.5 \pm 0.2^{\text{f}}$
Murray et al. [81] ^g	DSC	-	446.2	$18.3 \pm 0.4^{\text{f}}$
Tomassetti et al. [33]	DSC	-	447.1 ± 0.5	-
Ogasahara et al. [42]	DSC	-	-	$17.79 \pm 0.27^{\text{h}}$
Jacobs et al. [75]	DSC	>0.99	449.55	17.5
Torres et al. [36]	DSC	0.9999	448.9	18.1
Sabbah and Guardado [45]	DTA ^e	0.9999	448.4 ± 0.1	17.0 ± 0.2
Dabrowski et al. [82]	DSC	-	447.6 ± 0.1	17.49 ± 0.17
Lousada et al. [39]	DSC	-	447.73 ± 0.12^f	$17.81 \pm 0.06^{\text{f}}$
Rojas and Vieyra-Eusebio [65] ^g	DSC	0.9991	448.0 ± 0.8^f	$17.8 \pm 0.4^{\text{f}}$
This work ^g	DSC	0.9998	446.9 ± 0.3^f	$18.1 \pm 0.3^{\text{f}}$
Mean ⁱ			$447.3 \pm 1.3^{\text{f}}$	$17.9 \pm 0.7^{\text{f}}$

^a Mole fraction purity indicated if available.^b Indirect determination, $\Delta_{\text{cr}}^{\ell} H_{\text{m}}$ derived from the enthalpy measurements reported by the authors and the heat capacity data by Edwards and Kington [31]. Both data sets deviate from the heat capacity of the crystalline phase recommended in this work (see figure 2).^c DC = Drop calorimetry.^d DSC = Differential scanning calorimetry.^e DTA = Differential thermal analysis.

^f The expanded uncertainties quoted are twice the standard deviation of the mean.

^g Calibration of temperature and enthalpy explicitly described.

^h The authors reported the values $\Delta_{\text{cr}}^{\ell} H_{\text{m}} = (17.73 \pm 0.25) \text{ kJ mol}^{-1}$ and $(17.85 \pm 0.1) \text{ kJ mol}^{-1}$ for large and powdered crystals, respectively. Mean value is given.

ⁱ Only data indicated by bold font were used to calculate the mean value.

TABLE 9Standard molar thermodynamic functions in the ideal gaseous state at $p = 10^5$ Pa.^a

T/K	$C_{p,m}^{\text{g}0}$	$S_m^{\text{g}0}$	$\Delta_0^T H_m^{\text{g}0} / T$	$-\Delta_0^T G_m^{\text{g}0} / T$
(J·K ⁻¹ ·mol ⁻¹)				
200	104.7	318.2	63.6	254.6
250	133.8	344.6	74.7	270.0
273.15	148.0	357.1	80.3	276.8
298.15	163.4	370.7	86.6	284.1
300	164.5	371.7	87.1	284.7
400	221.5	427.1	113.8	313.3
500	267.3	481.7	140.1	341.6
600	302.6	533.7	164.4	369.3
700	330.2	582.5	186.1	396.3
800	352.4	628.0	205.6	422.5
900	370.8	670.6	223.0	447.7
1000	386.2	710.5	238.5	472.0

^a Calculated using the DFT B3LYP/6-311+G(2df,p) scaled frequencies and the 1-D HR scheme.

$\Delta_0^T H_m^{\text{g}0} / T \equiv (H_m^{\text{g}0}(T) - H_m^{\text{g}0}(0)) / T$ is the reduced enthalpy in the ideal gas state.

$-\Delta_0^T G_m^{\text{g}0} / T \equiv -(G_m^{\text{g}0}(T) - G_m^{\text{g}0}(0)) / T$ is the reduced Gibbs energy in the ideal gas state.

TABLE 10

Parameters of the Cox equation (4).

Phase	A_0	$A_1 \cdot 10^4$	$A_2 \cdot 10^8$	T^0	p^0/Pa	$(T_{\min} - T_{\max}) / \text{K}$
Crystalline	3.049675	-2.731970	2.165270	447.3	16750	242.0 – 447.3

TABLE 11Recommended vapor pressures and molar enthalpies of sublimation $\Delta_{\text{cr}}^{\text{g}}H_{\text{m}}$.^a

T/K	p/Pa	$\Delta_{\text{cr}}^{\text{g}}H_{\text{m}}/(\text{kJ}\cdot\text{mol}^{-1})$
242	$(8.6 \pm 0.9) \cdot 10^{-4}$	75.72 ± 0.38
250	$(2.9 \pm 0.3) \cdot 10^{-3}$	75.54 ± 0.38
260	$(1.2 \pm 0.1) \cdot 10^{-2}$	75.32 ± 0.38
270	$(4.2 \pm 0.3) \cdot 10^{-2}$	75.08 ± 0.38
280	0.139 ± 0.009	74.84 ± 0.38
290	0.419 ± 0.020	74.59 ± 0.38
298.15	0.974 ± 0.026	74.38 ± 0.38
300	1.172 ± 0.026	74.33 ± 0.38
310	3.060 ± 0.028	74.06 ± 0.38
320	7.499 ± 0.032	73.79 ± 0.38
330	17.35 ± 0.04	73.51 ± 0.38
340	38.10 ± 0.06	73.22 ± 0.38
350	79.75 ± 0.10	72.92 ± 0.39
360	159.8 ± 0.2	72.62 ± 0.40
370	307.5 ± 0.3	72.29 ± 0.42
380	570.1 ± 0.6	71.96 ± 0.44
390	1022 ± 1	71.61 ± 0.48
400	1773 ± 1	71.23 ± 0.52
410	2990 ± 2	70.83 ± 0.60
420	4906 ± 2	70.39 ± 0.70
430	7848 ± 3	69.91 ± 0.83
440	12263 ± 3	69.37 ± 1.02
447.3	16750 ± 4	68.94 ± 1.14

^a The stated uncertainties reflect the uncertainties in the selected input data for the SimCor method and the uncertainty in the description of the state behavior.

Figures and figure captions

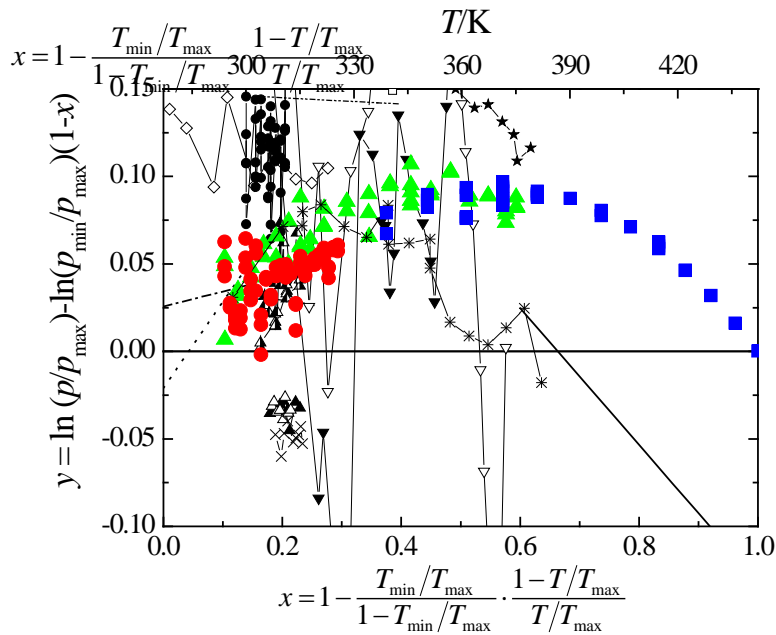


FIGURE 1. Arc representation of vapor pressure data. ” , Kaplan et. al. [70] ; ? , Edwards and Kington [72] (hole I); A , Edwards and Kington [72] (hole II); • , Andrews and Westrum [40]; 7 , Calado et al. [73] (larger hole), 8 , Calado et al. [73] (smaller hole); B , Pelino et al. [35] (run 1, partially displayed); C , Pelino et al. [35] (run 2, partially displayed); x , Jacobs et al. [75] (static method, partially displayed); — , Jacobs et al. [75] (mass effusion method); —, Jacobs et al. [75] (torsion effusion method); M , Torres-Gómez et al. [76]; , , Ribeiro da Silva and Monte [60]; 7 , Monte et al. [77]; ~ , Siddiqi and Atakan [78]; ‘ , Emel'yanenko et al. [79]; □ , Lousada et al. [39]; , , this work (ICT Prague); ! , this work (NIST). Smoothed data are displayed by lines, and experimental data are displayed by symbols, sometimes with a connecting line for clarity. Data listed in table 3, which are not displayed, are out of scale.

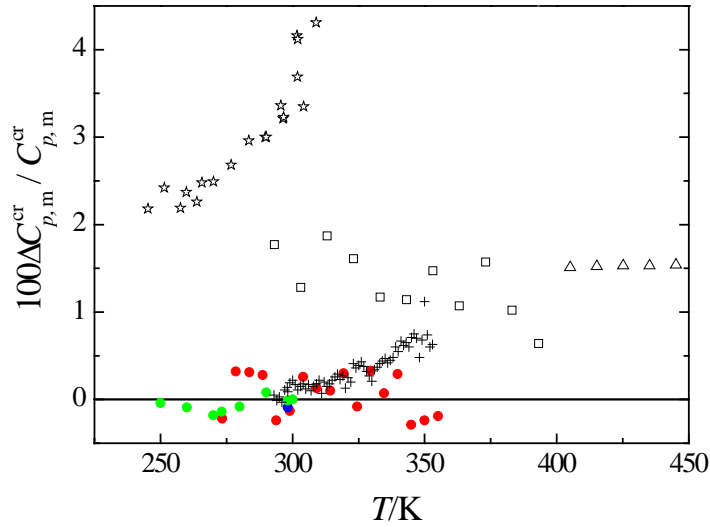
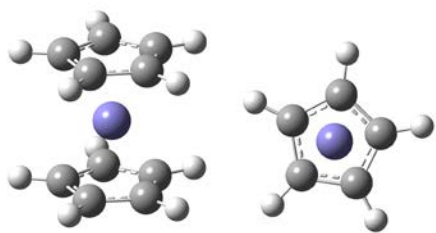


FIGURE 2. Relative deviations $\left[C_{p,m}^{cr}(\text{exp}) - C_{p,m}^{cr}(\text{calc}) \right] / C_{p,m}^{cr}(\text{calc})$ of the experimental heat capacities of the crystalline phase $C_{p,m}^{cr}(\text{exp})$ from the smoothed values $C_{p,m}^{cr}(\text{calc})$ obtained from equation (6). γ , Edwards and Kington [31]; δ , Joens and Gjaldbaek [32]; \square , Tomassetti et al. [33]; \triangle , Ogasahara [42]; \square , Rojas and Vieyra-Eusebio [65]; \bullet , This work (Calvet calorimetry, ICT Prague); \bullet , This work (drop calorimetry, University of Porto). Data sets displayed in color as solid colored circles were used in the development of equation (6).

Eclipsed conformation (D_{5h})



Staggered conformation (D_{5d})

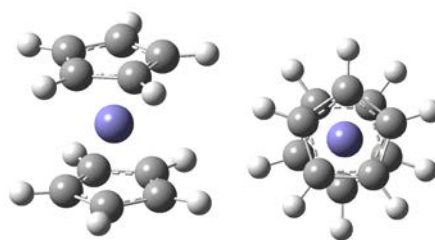


FIGURE 3. Two conformations of ferrocene.

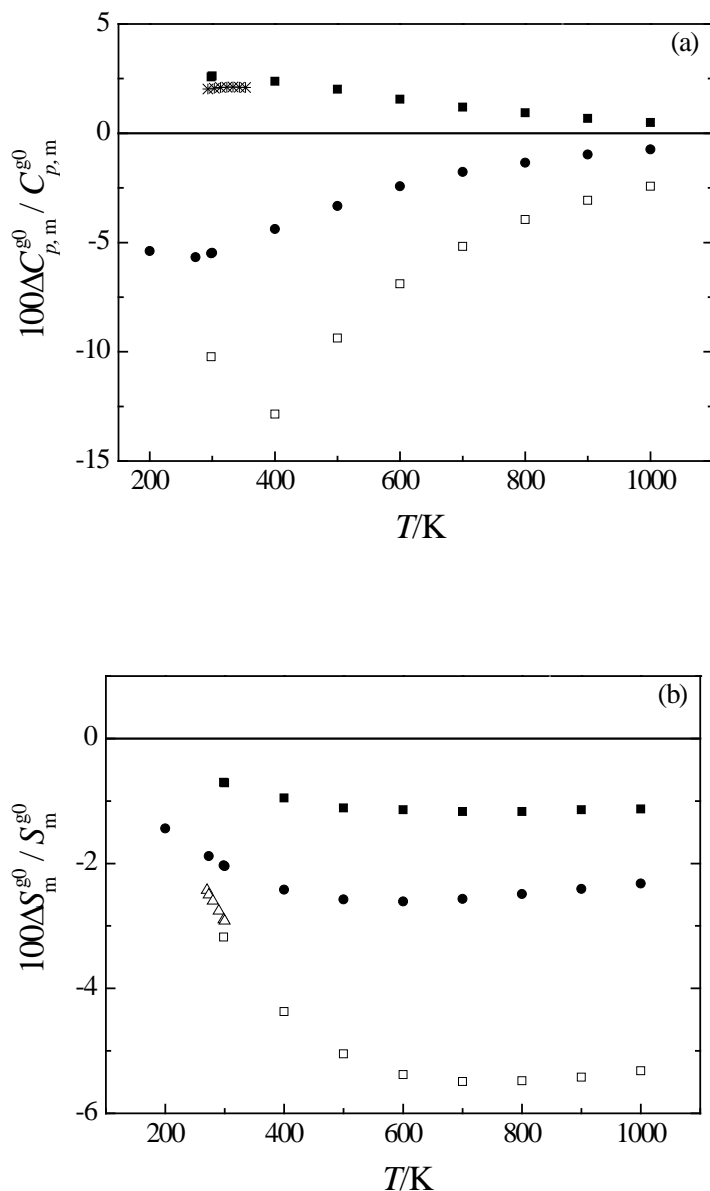


FIGURE 4. Relative deviations $[X(\text{lit}) - X(\text{this work})] / X(\text{this work})$ of the literature values of the ideal-gas thermodynamic properties from those calculated in this work (see table 9). (a) Ideal-gas heat capacities $X \equiv C_{p,m}^{g0}$. (b) Standard ideal-gas entropies $X \equiv S_m^{g0}$ ($p = 10^5$ Pa). ! , Lippincott and Nelson [62] (using experimental frequencies [46] and assuming free rotations of cyclopentadienyl rings); " , Turnbull [61] (using experimental frequencies [64] and assuming hindered rotation of cyclopentadienyl rings); ' , Rojas and Vieyra-Eusebio [65] (DFT, functional PW91, no other details are given, only $C_{p,m}^{g0}$ are reported); 8 , Adrews and Westrum [40] (using experimental frequencies [64] and assuming free rotation of

cyclopentadienyl rings, only $S_m^{g^0}$ reported) , , values calculated in this work using experimental frequencies [51] and 1D-HR formalism.

displayed); C , Pelino et al. [35] (run 2, partially displayed); x , Jacobs et al. [75] (static method, partially displayed); – , Jacobs et al. [75] (mass effusion method); —, Jacobs et al. [75] (torsion effusion method); M , Torres-Gómez et al. [76]; , , Ribeiro da Silva and Monte [60]; 7 , Monte et al. [77]; ~ , Siddiqi and Atakan [78]; ‘ , Emel'yanenko et al. [79]; □ , Lousada et al. [39]; , this work (ICT Prague); ! , this work (NIST); ” , this work (SimCor method); – , absolute deviations. Smoothed data are displayed by lines, and experimental data are displayed by symbols, sometimes with a connecting line for clarity. Some data listed in table 3 are not displayed because they are out of scale.

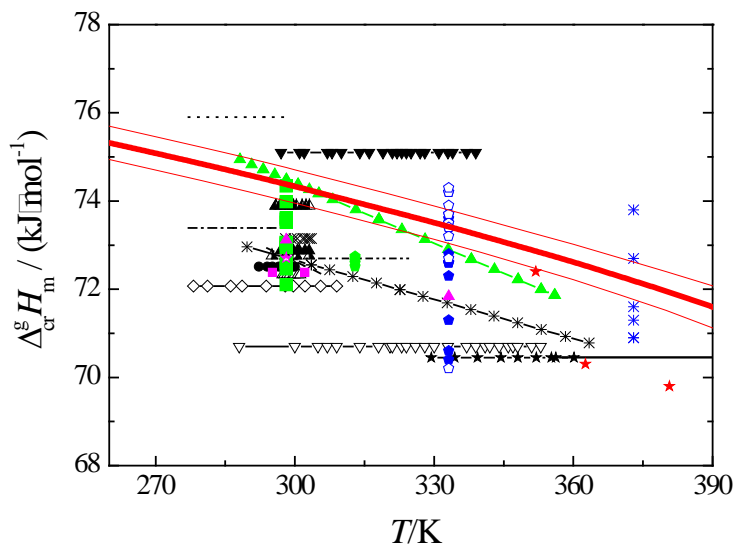


FIGURE 6. Comparison of sublimation enthalpies. Values derived from vapor pressure data: " , Kaplan et. al. [70] ; ? , Edwards and Kington [72] (hole I); A , Edwards and Kington [72] (hole II); • , Andrews and Westrum [40]; 7 , Calado et al. [73] (larger hole), 8 , Calado et al. [73] (smaller hole); B , Pelino et al. [35] (run 1); C , Pelino et al. [35] (run 2); x , Jacobs et al. [75] (static method); – , Jacobs et al. [75] (mass effusion method); —, Jacobs et al. [75] (torsion effusion method); M , Torres-Gómez et al. [76]; , , Ribeiro da Silva and Monte [60]; 7 , Monte et al. [77]; ~ , Siddiqi and Atakan [78]; ‘ , Emel'yanenko et al. [79]; □ , Lousada et al. [39]. Calorimetric values: ! , Edwards and Kington [72]; ! , Torres et al. [36]; 7 , Rojas-Aguilar et al. [37]; f , Kiyobayashi et Minas da Piedade [38]; ‘ , Santos et al. [29]; □ , Lousada et al. [39]; f , Rojas et and Vieyra-Eusebio [65] (DSC); „ , Rojas et and Vieyra-Eusebio [65] (Calvet calorimetry); x , this work (drop Calvet calorimetry). " , this work (SimCor method); – , uncertainty interval of the SimCor values. Some data listed in table 3 and 7 are not displayed because they are out of scale.

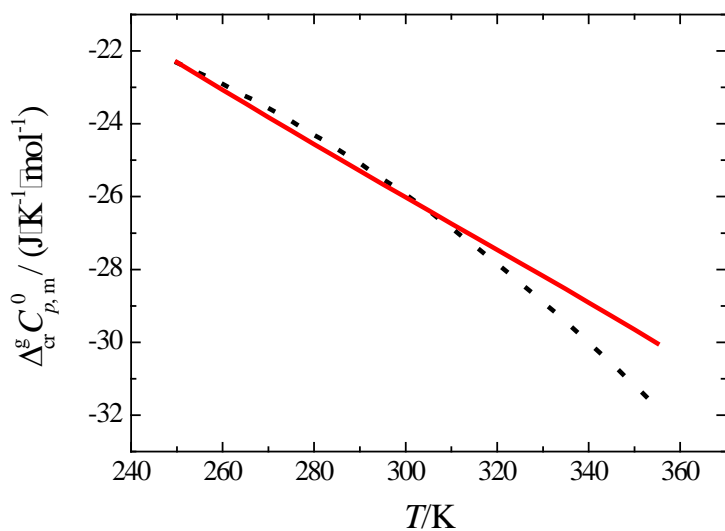


FIGURE 7. Comparison of the differences $\Delta_{\text{cr}}^g C_{p,m}^0 = C_{p,m}^{\text{g}0} - C_{p,m}^{\text{cr}}$ (—), $\Delta_{\text{cr}}^g C_{p,m}^0$ obtained from calorimetrically determined $C_{p,m}^{\text{cr}}$ (equation (6)) and calculated $C_{p,m}^{\text{g}0}$ (table 9); (---), $\Delta_{\text{cr}}^g C_{p,m}^0$ obtained from the SimCor method.